Journal Pre-proof

Production and characterization of bioaerogel particles from strawberries and their application as oil structuring ingredient in low-saturated fat cocoa spreads

Lorenzo De Berardinis, Stella Plazzotta, Lara Gibowsky, Baldur Schroeter, Daniel Alexander Méndez, Irina Smirnova, Lara Manzocco

PII: S0963-9969(25)01021-X

DOI: https://doi.org/10.1016/j.foodres.2025.116683

Reference: FRIN 116683

To appear in: *Food Research International*

Received date: 17 January 2025

Revised date: 14 May 2025

Accepted date: 17 May 2025

Please cite this article as: L. De Berardinis, S. Plazzotta, L. Gibowsky, et al., Production and characterization of bioaerogel particles from strawberries and their application as oil structuring ingredient in low-saturated fat cocoa spreads, *Food Research International* (2024), https://doi.org/10.1016/j.foodres.2025.116683

Production and characterization of bioaerogel particles from strawberries and their application as oil structuring ingredient in low-saturated fat cocoa spreads

Lorenzo De Berardinis[a], Stella Plazzotta[a], Lara Gibowsky[b], Baldur Schroeter[b], Daniel Alexander Méndez[c], Irina Smirnova[b], Lara Manzocco[a]

[a] Department of Agricultural, Food, Environmental and Animal Sciences, University of Udine, Via Sondrio 2/A, 33100 Udine, Italy

[b] Institute of Thermal Separation Processes, Hamburg University of Technology, Eißendorfer Straße 38, 21073 Hamburg, Germany

[c] Food Safety and Preservation Department, Institute of Agrochemistry and Food Technology (IATA-CSIC), Valencia, Spain

Abstract

Bioaerogels bear high potential in the development of fat-replacers, due to their oil-structuring capacity. However, current aerogel preparation from biopolymeric gels requires a complex and resource-intensive processes, which might limit their adoption as oil-structuring food ingredients. A simpler and more sustainable process to produce bioaerogels could be based on their direct preparation from plant tissues rather than from biopolymeric gels. Similar to gels, also in plant tissues, water is embedded into a fibrous network, so water removal while preserving tissue structure can lead to porous materials with bioaerogel properties, avoiding biopolymer extraction, purification and sol-gel steps. This work aimed to demonstrate the potential of tissue-derived aerogels as fat-replacement ingredients in cocoa spreads. To this aim, strawberry pulp was subjected to water-to-ethanol exchange, wet milling, and supercritical-CO_2-drying. This process resulted in bioaerogel particles with high mesopore volume (0.69 cm^3 g^{-1}), low density (0.03 g cm^{-3}) and high surface area (233 m^2 g^{-1}). The particles showed an oil absorption capacity higher than 90%, leading to a plastic material retaining 80% oil upon centrifugation. Strawberry bioaerogel particles were used to formulate low-

saturated fat cocoa spreads. A bioaerogel particle amount as low as 0.2-0.4 g/100 g_{spread} was enough to obtain spreads covering a wide range of rheological and spreadability properties. Preliminary techno-economic assessment demonstrated the technical and economic feasibility of the proposed process to produce bioaerogels from plant tissues intended as fat-replacement ingredients.

Key-words: supercritical drying; microstructure; porosity; oleogelation; colloidal mill

1. Introduction

An aerogel is an ultralight solid characterised by a high porosity (70.0 – 99.8%), significant specific surface area (up to 1200 m^2/g) as well as low density (0.003 – 0.5 g/cm^3) (Fricke & Tillotson, 1997). Aerogels can be produced from a variety of precursors (classically inorganic silica), where the organic ones, based on proteins or polysaccharides, have recently gained high interest (Abdullah et al., 2023). In fact, the derived materials, defined as bioaerogels, are biodegradable and biocompatible, and could therefore find large applications in environmental, biomedical, and food fields (Manzocco et al., 2021). As regards the food sector, different authors have reported the potential use of porous materials as active packaging materials able to extend food shelf-life. Such materials can indeed absorb unwanted substances responsible for food quality decay during storage. At the same time, their pores can easily host antimicrobial or antioxidant molecules that are then released in a controlled way, exerting a food protection role (Kurd et al., 2025; Wu et al., 2024). Aerogels have also been demonstrated to bear great potential as innovative food ingredients. These unique porous materials can be loaded with huge amounts of target compounds, which are protected by the aerogel scaffold during digestion, accounting for controlled bioactive and nutrient delivery through the diet (Kleemann et al., 2020; Plazzotta et al., 2022).

Thanks to their open-pore structure and high internal surface area, bioaerogels are able to absorb significant amounts of liquid oil (Manzocco et al., 2022; Ciuffarin et al., 2023). In this context, bioaerogels in the form of micrometric particles have been shown to present the ability to structure liquid oil upon simple mixing. This peculiar functionality is related to multiple mechanisms entailing

not only oil absorption into aerogel particle pores but also the establishment of a particle-particle network driven by weak interactions between the hydrophilic surface of biopolymeric aerogel particles in the hydrophobic oil environment (Plazzotta et al., 2020 and 2025). Oil structuring by aerogel particles can thus be used to prepare foods with physical behaviour (e.g., rheological properties, spreadability) comparable to those containing commercial hard fats but with an improved nutritional profile. Fats rich in unhealthy saturated fatty acids are actually substituted by liquid oils rich in unsaturated fatty acids (Jung et al., 2023). In this context, recent studies have exploited the oil structuring capability of bioaerogel particles in the formulation of foods with an improved lipid profile. In particular, Plazzotta et al. (2023, 2025) used whey and pea protein bioaerogel particles for the first time as fat replacers in the formulation of cocoa spreads. Cocoa spreads are products commonly containing up to 30-60 g/100 g of saturated-rich fats such as palm oil, coconut oil, and cocoa butter. Powdered ingredients including sugar, dairy-based powders (e.g., whey proteins) and cocoa powder are finely dispersed in the semi-solid fat crystalline network, which prevents sedimentation and phase separation while ensuring the characteristic spread rheological properties (Manzocco et al., 2014). The bioaerogel-based spreads exhibited comparable physical properties to those of commercial counterparts, yet with an improved nutritional profile, due to the reduction of the saturated fatty acid content.

Despite the huge potential of bioaerogels as fat-replacement ingredients, their complex, water- and energy-intensive production process could limit their widespread adoption in the food sector. The peculiar properties of bioaerogels are indeed the consequence of their production process, in which supercritical CO_2 drying (SCD) has a pivotal role in removing the solvent from an aqueous gel (i.e., hydrogel), thereby maintaining the original gel structure (García-González et al., 2019). Bioaerogels are conventionally obtained through a series of steps, beginning with the dissolution of a biopolymer in water, which is then gelled *via* different methods (*e.g.*, heat treatment, ionic or covalent crosslinking, non-solvent coagulation) to produce a hydrogel. Subsequently, the hydrogel is subjected to a gradual water-to-ethanol solvent exchange. This process results in the formation of an alcogel,

which is then subjected to supercritical-CO_2-drying, allowing the removal of the liquid phase without affecting the pore structure (Betz et al., 2012). In the supercritical state, CO_2 exhibits low viscosity and high diffusivity, forming a single phase with ethanol, and preventing the formation of liquid-vapor interfaces. Consequently, the absence of capillary forces in the biopolymeric network enables the production of bioaerogels with significant mesopore content (Andlinger et al., 2021).

The application of this bioaerogel production process entails the use of pure ingredients, like polysaccharides and proteins, which are obtained through energy- and resource-intensive pre-treatments and extraction procedures (Chaka, 2022). Moreover, a large amount of water is required to obtain the initial biopolymer solution, and high energy (commonly heat), as well as accurate process optimisation, are required to prepare the initial hydrogel, which should be able to withstand the subsequent water removal phases. To make the process simpler and more sustainable, in their pioneering work, Plazzotta et al. (2018) suggested that bioaerogels could be directly prepared from cheap and widely available plant tissues, skipping the extraction, purification, and gelation steps, and avoiding inefficient water cycles. This approach to the development of aerogels stems from the observation that plant tissues could be regarded as intricate moisture-rich polymeric frameworks, primarily structured by cellulosic fibres and proteins organised in cell walls, housing water within intra- and inter-cellular spaces (Plazzotta et al., 2018). The removal of water, while preserving cellular integrity, may potentially yield an aerated and partly mesoporous structure. To date, only a few works have investigated the direct conversion of plant tissues into bioaerogels. Specifically, these works focused on by-products of the food industry, currently downcycled to the production of biofuel or compost, such as lettuce leaves discarded during fresh-cut production (Plazzotta et al., 2018), apple pulp generated during juice extraction, spent ground coffee (Gaggero et al., 2022) and substandard seeds discarded by the pea canning industry (Manzocco et al., 2024). More recently, Gibowsky et al. (2025) showed that a wide range of aerogel-like microstructures can be obtained by simply changing the starting vegetable material. In all this case, bioaerogel particles showed a remarkable oil absorption capacity, in the same range as that of bioaerogels produced from pure biopolymers, such

as whey or pea proteins. Nevertheless, oil absorption capacity was shown to be generally higher for bioaerogels derived from water-rich tissues (Gibowsky et al., 2025). For instance, bioaerogel from lettuce leaves showed oil absorption capacity higher than that obtained from peas. It should be noted that peas have a dense structure embedding carbohydrates, proteins, and lipids, accounting for their biological function of nutrient and energy storage (Wu et al., 2023). By contrast, lettuce leaves primarily serve for photosynthesis, which occurs in the presence of large vacuoles filled with water (~ 96 g/100 g) to maintain plant turgidity (Laxar, 2003). Differences in oil absorption capacity of plant-derived bioaerogels could be thus the result of the different structural organisation of the plant tissue, which would affect the porosity of the aerogel and its performance.

In the light of these scientific suggestions, more information is certainly needed to widen the knowledge of plant tissue-derived bioaerogels intended as oil-structuring ingredients for fat replacement. The aim of this work was thus to prepare and characterise aerogel particles from strawberry tissue, demonstrating their potential as ingredients for fat replacement in cocoa spreads. Strawberries actually contain high water content (> 90 g/100 g) (Agudelo-Laverde et al., 2013) and peculiar tissue structure, mainly composed by parenchymatic cells with thin-walled cells rich in water, embedding vascular tissues characterised by long fibres (Suutarinen et al., 2000). Moreover, strawberries are indeed highly fragile and susceptible to damage during industrial processing, making their conversion into bioaerogel particles an interesting strategy to reduce and valorise their potential waste (Sharma & Venugopal, 2023). Based on these considerations, strawberries were subjected to water-to-ethanol solvent exchange and wet milling. The obtained strawberries alcogel particles were then collected and dried by supercritical-CO_2. Supercritical dried particles were characterised in terms of composition, microstructure, physical properties (density, specific surface area, and mesopore volume), and oil structuring capacity (oil holding capacity, confocal microscopy, rheological and spreadability properties). The applicability of strawberry bioaerogel particles as an ingredient for cocoa spreads with low saturated fat content was then assessed, along with their techno-economic feasibility.

2. Materials and Methods

2.1 Preparation of supercritical dried strawberry particles

Fresh strawberries were purchased at a local supermarket and processed without further storage time. The calyx was removed and the pulp was subjected to shredding (500 g pulp in 0.5 L distilled water) in a kitchen mixer (Bosch Stand Blender MMB6174S VitaPower). The shredded pulp was washed repeatedly (three times) with 10 L of distilled water under slight stirring via overhead stirrer (250 rpm, Phoenix Instrument RSO 20A equipped with a four-blade agitator with rectangular, flat blades with 2 cm length and 1 cm height), to remove water-soluble components. All washing and shredding steps were carried out at 20 °C under open air. Subsequently, samples were transferred into pure ethanol (EtOH, 99.9 g/100 g, denatured, Carl Roth GmbH & Co. KG) for solvent exchange at 20 °C, until a minimum final concentration of 97.0 g/100 g EtOH in the liquid phase was achieved (controlled by density measurements, Anton Paar, DMA 4500 M). Approximately 10 L of EtOH per L pulp were used. The solvent exchanged samples (alcogels) were then further grinded down by wet-milling process, using a colloid mill (IKA magic LAB, milling speed = 22000 rpm, gap width = 900 µm) according to Schroeter et al. (2023). Obtained microparticles were sealed into filter paper bags and transferred to an autoclave (3.9 L volume) for drying with supercritical-CO_2. The supercritical-CO_2-drying was performed at a pressure of 120 bar and a temperature of 40 °C. A continuous flow of CO_2 (120 - 140 g min^{-1}) was set until complete extraction of EtOH was achieved (3 h). After slow depressurization (2 bar min^{-1}) samples were collected and stored in sealed vessels in a desiccator over calcined silica gel until further use/analysis.

2.2 Preparation of cocoa spreads

Cocoa spreads were prepared according to a two-step mixing procedure (Plazzotta et al, 2023), as shown in Figure 1. Specifically, a composition simulating that of commercial spreads was considered, resulting in a control formulation consisting of 7 g/100 g_{spread} of whey protein isolate powder (WPI), 10 g/100 g_{spread} of cocoa powder, 53 g/100 g_{spread} of icing sugar, and 30 g/100 g_{spread} of hard fat (e.g., palm oil). Cocoa spreads were thus prepared by partially replacing the WPI with increasing amounts

of bioaerogel particles (from 0 to 1.6 g/100 g_{spread}) and completely replacing the hard fat with sunflower oil. To this aim, the bioaerogel particles were manually mixed with oil by using a laboratory spatula for about 60 s, until the mixture was visually homogeneous. Following, cocoa powder and icing sugar were added and further mixed until a homogeneous spread was obtained (Plazzotta et al., 2023). The obtained spreads were stored in sealed sample holders at room temperature, in the dark, for up to 1 month.

2.3 Carbohydrate composition

The sugar composition of supercritical dried strawberry microparticles was determined as previously described after acidic methanolysis (Méndez et al., 2023). Samples (1 mg) were freeze-dried and incubated with 1 mL of 2 M HCl in dry methanol for 5 h at 100 °C. Subsequently, samples were neutralized with pyridine, dried under a stream of air, and hydrolysed further for one hour with 2 M trifluoroaceticacid at 100 °C. After repeated drying under a stream of air, samples were re-suspended in milliQ, filtered, and injected. Monosaccharides were analysed using high-performance anion exchange chromatography with pulsed amperometric detection (HPAEC-PAD) with an ICS-6000 system (Thermofisher) equipped with a CarboPac PA1 column (4 × 250 mm, Dionex). Control samples of known concentrations of mixtures of glucose, fucose, rhamnose, galactose, arabinose, xylose, mannose, galacturonic acid, and glucuronic acid were used for calibration (Merck, Germany). The cellulose content was estimated as the difference between methanolysis and Saeman hydrolysis glucose content (Saeman, 1945). In brief, 1 mg of each sample previously freeze dried was incubated with 0.125 mL of sulfuric acid during 3 hours at room temperature, then 1.375 mL of milliQ water was added and the samples were sealed and heated during 3 hours at 100 ºC. The sample was filtered and diluted 1:10 with milliQ water, then injected using the same equipment of the methanolysis method described previously. Calibration was performed using control cellulose with known concentrations (Merck, Germany).

2.4 Protein content

The protein content was determined by the Dumas combustion method (nitrogen conversion factor 6.25) according to ISO/TS, 16634–2 (2016).

2.5 Ash content

The ash content was determined in triplicate *via* thermogravimetric analysis (Linseis TGA PT 1600). An amount of 20 to 40 mg of sample was placed in an aluminium oxide crucible and heated up to 850 °C (with a heating rate of 10 °C min^{-1}) under an oxidised atmosphere. The final temperature was maintained for 120 min to ensure complete conversion of the organic part. The ash content of the sample was then calculated by dividing the remaining mass by the initial mass.

2.6 Bulk density

Bulk (untapped) density of strawberry microparticles was estimated using a graduated cylinder with a volume of 11.5 cm^3. Particles were filled in the cylinder without tapping and bulk density was calculated as a ratio of the particles weight and the occupied volume.

2.7 Nitrogen physisorption

The specific surface area and mesopore size distribution of bioaerogels were evaluated *via* nitrogen physisorption using a Nova 3000e Surface Area Analyzer from Quantachrome Instruments. The specific surface area of samples was evaluated based on the Brunauer-Emmett-Teller method (BET) in the p/p_0 range of 0.03-0.27. The Barrett-Joyner-Halendia (BJH) method was used to estimate the mesopore volume (V_{meso}) and the pore size distribution. Measurements were carried out three times with individual samples.

2.8 Appearance

Sample images were captured using an image acquisition cabinet (Immagini & Computer, Bareggio, Italy) fitted with a digital camera (EOS 550D, Canon, Milan, Italy). The camera was set up on a flexible stand, positioned 50 cm above a black cardboard base on which the samples were positioned. Illumination was achieved using 4 × 100 W frosted photographic floodlights, arranged to reduce

shadow and minimize glare. Images were imported in jpeg format using the software EOS Utility 2.14.20.0 (Canon, Milan, Italy).

2.9 Confocal microscopy

Fast Green and Nile Red 0.2% (w/w) aqueous solutions (Sigma Aldrich, Milan, Italy) were used to stain proteins and oil, respectively, while a 0.01% aqueous solution of Brightener (Sigma Aldrich, Milan, Italy) was used to stain fibres. The solutions were added to structured oil or cocoa spread, and manually mixed. The samples were then placed on the microscope slide, covered with a cover slide, and examined using a confocal laser scanning microscope at 100 × magnification (Leica TCS SP8× confocal system, Leica Microsystems, Wetzlar, Germany). Images were imported in jpeg format using the software LasX 3.5.5 (Leica Microsystems, Wetzlar, Germany). Attribution of physical elements observed in the images to different spread components was performed based on comparison with literature data (Rousseau et al., 2015).

2.10 Scanning electron microscopy

Imaging of the bioaerogel samples was carried out *via* scanning electron microscopy (SEM, Zeiss Supra VP55, Jena, Germany). Samples were sputtered with a conductive, thin layer of gold before analysis (thickness approx. 6nm, Sputter Coater SCD 050, BAL-TEC). Measurements were performed under a high vacuum at an accelerating voltage of 3 kV using a SE2- detector at a working distance of 3.9 mm.

2.11 Oil structuring capacity

The procedure proposed by Alavi & Ciftci (2023) was used, with some modifications. Specifically, bioaerogel particles were ground with an analytical mill (8010EB, Warning Commercial, Torrington, Connecticut) two times for 20 s and transferred in a glass beaker. Sunflower oil was then gradually added in increasing bioaerogel:oil weight ratio (1:10, 1:20, 1:30, 1:40), under continuous manual mixing. Samples were prepared in duplicate and stored in sealed specimen holders, in the dark at 25 °C until use.

2.12 Oil holding capacity

An amount of about 1 g of structured oil or cocoa spread was weighed in a 2 mL Eppendorf, and centrifuged (Mikro 20, Hettich Zentrifugen, Tuttlingen, Germany) at 15,000 g for 15 min at 4 ºC. At the end of centrifugation, the oil released was carefully removed using an absorbent paper, and the sediment weighed (P_2). The oil holding capacity (OHC) was calculated as g of oil held by 1 g of bioaerogel particles, using the following eq. (1):

$$OHC\ (\%) = \frac{\text{Oil released (g)}}{\text{Total oil (g)}} \times 100 \quad (1)$$

2.13 Rheological properties

The viscoelastic properties (moduli G′, G″ and tan δ) of samples were assessed with an RS6000 Rheometer (Thermo Scientific RheoStress, Haake, Germany). The rheometer was equipped with a Peltier system for temperature control. Measurements were conducted using a parallel plate geometry at 20 °C with a gap of 2.0 mm. Oscillatory sweep tests were executed to identify the linear viscoelastic region (LVR), increasing stress from 1 to 10^6 Pa at 1 Hz frequency. Critical stress (Pa) was identified as the strain value corresponding to a 10% drop in G′ value.

2.14 Spreadability

Spreadability was evaluated using a 34TM-5 Instron machine equipped with a back-extrusion food cell (S5405A, Instron). The apparatus comprised a moving head and a cup, the latter was filled with 25 g of the sample. The sample was subsequently compressed by 5 mm using the head at a speed of 25 mm/s, upon an auto-detected force of 1 N, and stress was registered as a function of compressive strain.

2.15 Techno-economic feasibility

A team-based approach was conducted in partnership with an industrial manufacturer of inorganic aerogels to assess the technical and economic feasibility of producing strawberry bioaerogels. The investigation was structured through three sequential phases: (i) a technical audit of operational workflows at the company production facility, including resource consumption metrics (*i.e.*, ethanol,

supercritical CO_2, energy) and solutions aiming to reduce their consumption; (ii) step-by-step sessions with the R&D team to assess technical constraints in adapting the existing infrastructure and procedures for inorganic aerogel production to the industrial production of plant-tissue derived bioaerogels; (iii) cost modelling through interviews with production specialists, integrating variable (raw materials, energy) and fixed (equipment retrofitting) costs.

2.16 Data analysis

Analyses were conducted in triplicate on at least duplicate samples, and the results are presented as mean values with standard deviations. Statistical analysis was performed on OHC data using R v. 2.15.0 (The R Foundation for Statistical Computing). Bartlett's test was used to assess the homogeneity of variance. One-way ANOVA was conducted, followed by Tukey's post hoc test to identify statistically significant differences among the means ($p < 0.05$).

3. Results and discussion

3.1 Physical properties of strawberry bioaerogel particles

Processing of strawberry pulp *via* washing, solvent exchange, wet-milling, and SCD resulted in a light, fine, and odourless powder. The break-up of samples during the milling step led to irregular-shaped sample shreds with a maximum size of a few hundred micrometres (Figure 2**, a**). Notably, the samples lost almost all of their intrinsic colour (Figure 2**, a**, inset), attributed to the extraction of anthocyanins, which are well soluble in water and polar organic solvents (Taghavi et al., 2023). Hereby, pigment leaching was indicated to be most pronounced during the solvent exchange step, since the EtOH/water solution turned red, while pronounced discolouration of the pulp occurred.

Most other water-, ethanol- and CO_2-soluble phytochemicals are also expected to be removed during processing, due to the numerous washing/extraction steps. Solid remains should therefore be mainly comprised of cortical cell wall components. The latter are typically built up by crystalline cellulose microfibrils and co-extensive pectin networks surrounded by an amorphous matrix of polysaccharides, such as pectin, lignins, and hemicelluloses, along with proteins and inorganic

molecules (Brummell, 2006; Castro et al., 2021; Suutarinen et al., 1998). Composition analysis of the dried products revealed indeed, that 71.8 % of the organic, solid fraction is composed of usual cell-wall material (Table 1). Besides pectin, proteins, and cellulose, a significant monosugar content was also detected, which was most probably formed by partial decomposition of easily hydrolysable biopolymer fractions during acidic treatment in the composition analysis. While a high pectin content of up to ~ 50% is typical for fruit cells, hemicellulose, and lignin components are expected to be the main parts of the remaining fraction (non-identified components, n.d. in Table 1) (Brummell, 2006).

Table 1. Composition (cellulose, pectin, monosugars, proteins, and ashes) and physical properties (bulk density, ρ_b, specific surface area, S_v, and mesopores volume, V_{meso}) of strawberry bioaerogel particles. % is related to the overall soluble sample fraction.

Cellulose (%)	**Pectin (%)**	**Monosugars*** **(%)**	**Proteins (%)**	**n. d.**** **(%)**	**Ashes***** **(%)**	**ρ_b ***** **(g cm^{-3})**	**S_v (m^2 g^{-1})**	**V_{meso} (cm^3 g^{-1})**
12.1 ± 0.5	49.3 ± 3.4	4.5 ±0.5	12.9 ± 0.2	28.1	1.4 ± 0.5	0.03	233.3 ± 5.3	0.69 ± 0.14

* contain glucose, glucuronic acid and mannose ** non identified, soluble fraction *** regarding the overall dry weight of the sample

**** standard deviation lower than balance accuracy

The bulk density (Table 1) was in the common range for biopolymer aerogels and points towards a high overall porosity. Since the determination of ρ_b is based on the non-compressed bed of particles, the volume provided by interparticle voids contributes to the overall result and the bulk density is a rather rough estimate. A more detailed analysis of the microstructural properties is provided by combined results of nitrogen physisorption and SEM imaging. In SEM images of lower magnification, folded and amorphous sample parts are visible, which are most likely outer cell wall remains (Figure 2**, b**). Results show that the macroscopic cellular structure was largely deformed during processing (e.g., due to mechanical forces occurring in the shear-head of the colloid mill during wet-milling). In addition, fibrous and differently branched porous structures are visible, which originate from fibrillar tissue components (e.g., cellulosic and pectin-based inner cell wall structures) and form macro- to mesoporous networks (Figure 2**, b-d**). Based on SEM pictures, the diameters of the according fibres were estimated to be in the range of approx. 11 – 28 nm. Even smaller mesopores

with a few nanometres in diameter are also detected in high-resolution SEM images (Figure 2**, d**, inset**)**. It has to be pointed out, that highlighted regions are chosen parts of an – from a microstructural point of view – inhomogeneous sample which also contains non-porous parts.

To quantify the contribution of different sized mesopores, nitrogen physisorption was performed. The according isotherm shows a type IV hysteresis with steep increase at higher p/p_0 values (H3 shape), which is typically observed for many mesoporous bioaerogels, which also exhibit macropores (Figure 2**, e**) (Thommes et al., 2015). The pore size distribution consequently covers the whole mesoporous range (pore diameters of 5 – 50 nm) as well as small macropores (Figure 2**, f**) (Thommes et al., 2015). Considering the non-uniform nature of the samples and the different pore structures visible in the SEM images, it is interesting to estimate which types of pores primarily contribute to the specific surface area. We suggest, that small mesopores with pore diameters ≤ 12 nm and a high surface-to-volume ratio provide the most significant part of the internal surface, since they make up for approx. 20% of the overall detected mesopore volume (see inset, Figure 2**, f**). While nitrogen physisorption results are largely consistent with results obtained *via* SEM imaging, it is emphasized, that smaller micropores (pore diameter < 2 nm) and larger macropores are not being captured, and BJH-based pore size distributions represent therefore only a part of the overall multiscale-porous sample (Horvat et al., 2022). The specific surface area is overall in the same range as values found so far for other supercritically dried natural tissues based on apple pulp, spent ground coffee (~ 208 - 229 $m^2 g^{-1}$) and exceeds those of based on salad leaves (~ 100 $m^2 g^{-1}$). In summary, the results demonstrate the significant contribution of mesoporous part in the sample to the overall properties and the bioaerogel characteristics of the material.

3.2 Oil structuring ability of strawberry bioaerogel particles

Given the high porosity and surface area of strawberry bioaerogel particles, their oil structuring ability was evaluated to explore possible applications in the formulation of fat analogues. The appearance of the sample obtained by mixing strawberry bioaerogel particles with increasing oil amounts is shown in Table 2.

Table 2. Appearance of strawberry bioaerogel particles mixed with increasing sunflower oil amounts.

Oil content (g/100 g)	**91**	**95**	**97**	**98**
Appearance				

Upon the initial addition of oil, the strawberry-oil matrix exhibited a granular texture, characterized by the formation of small aggregates within a discontinuous network. During this phase, oil was mainly driven into the bioaerogel pores by capillary forces, with minimum surface interaction among particles (Selmer et al., 2019). As the oil content increased, the system exhibited enhanced structuration with the formation of larger aggregates and further establishment of a continuous network. This phenomenon can be attributed to the tendency of the oil to remain attached onto the surface of the bioaerogel particles, facilitating the formation of oil bridges among them. This, in conjunction with the hydrophilic interactions between the strawberry particles in a lipid environment, resulted in the formation of a continuous network. In fact, when hydrophilic particles are dispersed in a hydrophobic medium, they exhibit a propensity to form superficial interactions, resulting in the establishment of a particle-particle network (De Vries et al., 2017). However, an excessive amount of oil finally resulted in the loss of the network continuity among particles (Table 2). In other words, the dilution of strawberry bioaerogel particles in the oil media weakened the network, probably preventing proper surface interaction among them. This behaviour is consistent with the findings reported in other studies (Ciuffarin et al., 2024; Jung et al., 2023).

The strawberry bioaerogel demonstrated an exceptional capacity for oil absorption, resulting in materials containing more than 90% oil by weight, which is in line with the data of bioaerogel obtained from plant tissues rich in water like lettuce leaves (Plazzotta et al., 2018), and significantly higher than that of bioaerogels obtained from pure ingredients like whey and potato protein isolates (70% to 84%). The high oil absorption capacity observed in bioaerogels from plant tissues has been

attributed to their unique response to the aerogelation process, which has been shown to cause the expansion of the cellular structure (Plazzotta et al., 2018). The high oil absorption shown in Table 2 suggested that even in the case of strawberry tissues, the proposed aerogelation process probably did not impair the original elasticity of plant cells (Braybrook, 2015), which probably expanded during oil absorption. To further investigate this hypothesis, the sample containing 97 g/100 g of oil, characterized by a continuous self-standing structure, was selected for confocal microscopy analysis. The confocal micrograph (Table 3) showed the occurrence of fibrous and branched structures of strawberry bioaerogel corresponding most likely to the pectin fraction in the aerogel (in black and fluorescence), finely distributed in the oil (in yellow), which was entrapped within and between the strawberry fibrils. Moreover, small roundish black particles were observed, probably referring to the strawberry achenes broken during the colloidal mill process. A comparison of the bioaerogel structure before (Figure 2) and after (Table 3) oil absorption suggests that the fibrous structure of the bioaerogel particles swelled upon contact with oil, largely increasing the volume available for oil absorption. This large amount of oil was also demonstrated to be strongly held into the bioaerogel structure, as shown by the high OHC values (Table 3), which resulted in line with those of bioaerogels obtained from pure ingredients (Jung et al., 2023; Plazzotta et al., 2020, 2021). It could be inferred that the pectin-protein surface of the bioaerogel particles engaged in the formation of strong interactions with the oil, as also observed in emulsions stabilized with watermelon rind pectin (Mendez et al., 2021). The mixture of strawberry particles and oil (97 g/100 g) was submitted to the assessment of rheological properties (Table 3).

Table 3. Confocal micrograph, elastic modulus (G'), viscous modulus (G''), and loss tangent (tan δ) of the system containing strawberry particles and 97 % (w/w) of oil. Yellow = oil, Fluorescence and black = strawberry bioaerogel.

Confocal microscopy	OHC (%)	$G' \times 10^4$ (Pa)	$G'' \times 10^4$ (Pa)	tan δ

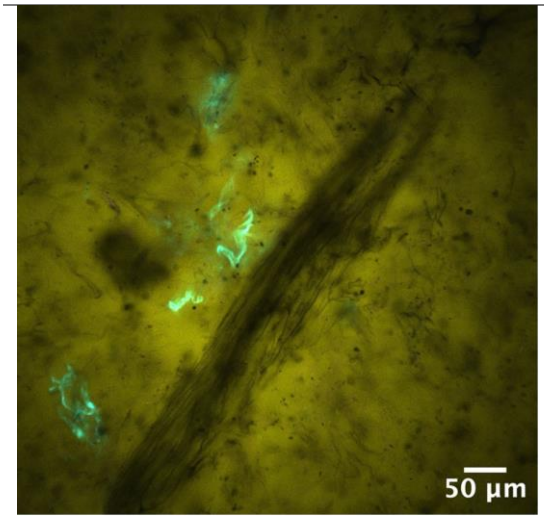	80 ± 1	2.07 ± 0.46	0.12 ± 0.02	0.06 ± 0.01

From the rheological point of view, this system presented a strong gel behaviour indicated by the independence of the elastic and viscous moduli (G′ and G″, respectively) in a frequency range from 0 to 15 Hz. Moreover, the low loss tangent (tan δ) value indicated an elastic behaviour, in agreement with the rheological properties of pure biopolymer oleogels obtained from bioaerogel particles (Plazzotta et al., 2021). Even if the latter demonstrated a lower oil absorption capacity than the strawberry ones, no significant differences in terms of rheological properties could be observed (Plazzotta et al., 2020, 2021), so that the material obtained from strawberry tissue (Table 3) presented properties comparable to those of commercial hard fat (*e.g.*, butter, palm oil, margarine, laminating shortening) (Blake & Marangoni, 2015), making it a possible candidate for fat-replacing in food formulations.

3.3 Cocoa spreads containing strawberry bioaerogel particles

The last part of the present work deals with the application of strawberry bioaerogel in the preparation of cocoa spreads with low saturated fatty acid content. To this aim, the strawberry bioaerogel particles were used to gradually replace whey protein isolate (WPI) powder in cocoa spreads while the reduction in fatty acid content was achieved by the use of sunflower oil as a lipid phase, excluding any addition of saturated fats such as palm or coconut oil. Table 4 reports the appearance and the OHC of the obtained spreads.

Table 4. Appearance and oil holding capacity (OHC) of cocoa spreads obtained by adding increasing content of strawberry bioaerogel.

Bioaerogel (%)	**0**	**0.2**	**0.4**	**0.8**	**1.2**	**1.6**
Appearance						
OHC (% w/w)	81.1 ± 3.0 ^{d}	89.9 ± 1.1 ^{c}	89.9 ± 1.1 ^{cd}	95.5 ± 0.6 ^{bc}	98.6 ± 0.3 ^{a}	99.8 ± 0.1 ^{a}

$^{a-c}$: means indicated by different letters are statistically different ($p<0.05$)

The control samples containing WPI exhibited a semi-liquid consistency whereas with the increase in bioaerogel content, the spreads transitioned into a self-standing system. The increase in the strawberry bioaerogel content thus resulted in a higher structuration of the spreads, as further confirmed by the increase in OHC values. Nevertheless, an excess in bioaerogel content (*i.e.*, 1.6 g/100 g_{spread}) caused the loss of the network continuity of the spreads, which presented a grainy and uneven morphology. This was probably caused by the excessive oil absorption by the bioaerogel particles, which reduced oil mobility and thereby impacted both the flowability and the homogeneity of the spreads (Rincon Cardona et al., 2013).

To enhance the comprehension of cocoa spreads microstructure, confocal microscopy analyses were conducted on cocoa spreads containing 0.2 and 0.4 g/100 g_{spread} strawberry bioaerogel, which appeared both as smooth and continuous spreads (Table 4). A comparison of the microstructure was made with the sample containing only WPI particles, referred to as control (Figure 3).

The microstructure of the spreads revealed a continuous oil phase (in yellow) embedding the different particles (*i.e.*, sugar, cocoa, protein, and bioaerogel), which contributed to the formation of a network due to their hydrophilic nature (Rousseau et al., 2015), thereby defining the structure of the spreads. Focusing on the particles, it was possible to distinguish WPI particles coloured in magenta, sugar crystals in black with a dimension up to 50 µm, and cocoa powder in fluorescence with a roundish shape (Rousseau et al., 2015). Strawberry bioaerogel particles also appeared in fluorescence, but presented larger size and more complex shapes.

Although all spreads appeared equally crowded with particles, significant differences between the samples were observed. Specifically, whey proteins were homogeneously distributed in the control sample (0 g/100 g_{spread} of bioaerogel) and principally adhered to the sugar crystals due to their chemical affinity. As expected, a decrease in these particles was obviously detected upon their progressive substitution with bioaerogel ones. The latter promoted the presence of larger protein structures, likely associated with the proteins characterizing the strawberry bioaerogel. Additionally, as the bioaerogel content increased, distinct fragments of strawberry cells became clearly visible, and evenly distributed throughout the sample. These fragments were recognisable by the presence of structural elements typical of vegetable cells (*e.g.*, tracheids, white arrow) or particularly irregular in shape (white circle). It is thus likely that such a wide range of complex particles would contribute to increase the interactions among solid particles in the spread, supporting the formation of a stronger continuous network. To further investigate the structuring effect of strawberry bioaerogel particles, the rheological properties of the spreads were characterised (Figure 4). It must be noted that the rheological attributes are of pivotal importance for cocoa spreads since they are associated with the typical solid-like behaviour and spreadability properties of these products. The amplitude sweep test showed how all the samples presented a gel-like behaviour with G' > G" at low shear stress (Figure 4A). With the increase of stress, the critical value was reached, determining the drop in elastic response (De Graef et al., 2011). The increase in bioaerogel content increased the elasticity (G') and the critical stress of the spreads, confirming the oil structuring ability of bioaerogel particles (Table 4). This observation confirms that the increase in strawberry bioaerogel content increased the particle-particle interactions enhancing the deformation resistance of the network formed within the oil matrix. This result is in agreement with data obtained by performing spreadability tests (Figure 4B), which give indications on the propensity of the samples to be spread (Kikini & Dickie, 1982) and is linked to consumer perception and appreciation of the product (Guichard et al., 2018). All samples exhibited the characteristic stress-strain profiles of a spreadable material, as described by an initial increase in stress with compressive strain, followed by a gradual reduction in the stress dependence

on strain, indicating the onset of flow (Guichard et al., 2018). The presence of increasing amounts of strawberry bioaerogel particles caused a shift of the curves towards higher values, as well as the occurrence of bumps in the curves (Figure 4B), which is associated with a higher force required to spread the sample and to the rupture of spread continuity during the test, respectively, indicating, overall, a reduction in spreadibility.

3.4 Techno-economic feasibility of large-scale production of bioaerogel from plant tissues

An evaluation was conducted in partnership with a leading industrial manufacturer of inorganic aerogels (mainly from silica) to obtain preliminary data on the technical and economic feasibility of the proposed process for developing bioaerogels from plant tissues.

During the audit in the company, no technical issues emerged in the adaptation of the considered industrial plant from inorganic aerogel production to the production of bioaerogels from plant tissues. On the opposite, this adaptation would highly simplify the production process since not requiring steps which are mandatory for inorganic aerogel production (e.g., hydrolysis and gelation). The audit also revealed that, differently from a lab-scale plants, industrial ones are equipped with solvent recycling systems, able to recover up to 98% of the ethanol and of the CO_2 used during the production process. Economic analysis of large-scale bioaerogel production was also performed even if detailed data are not disclosed in the present paper, due to their sensitive nature. Nonetheless, this analysis revealed that the adaptation of the existing inorganic aerogel production process to the production of plant-tissue derived bioaerogels would involve analogous capital investment but lower operational costs due to the elimination of specific processing steps and lower cost of plant-tissues compared to highly pure compounds. Collected data allowed for defining a tentative selling price of strawberry bioaerogel particles, which resulted in the range of many food ingredients commonly used for oil-structuring purposes (2-10 €/kg), yet allowing for a reasonable commercial margin.

4. Conclusions

In the present study, bioaerogel particles were successfully produced directly from strawberry tissues. The high water content and peculiar structure of strawberries enabled the production of a bioaerogel with a high porosity and extensive surface area, thereby allowing the absorption of significant quantities of oil. The production of bioaerogels directly from plant tissues dodges the necessity for the high-energy and resource-intensive processes commonly required for bioaerogels obtained from pure ingredients. This approach could be employed to enhance the sustainability of both bioaerogel production and the agri-food chain.

The developed bioaerogel particles were utilized in the development of low-saturated-fat cocoa spreads that demonstrated rheological and spreadibility properties comparable to those of commercial spreads high in saturated fats, yet with a significant improvement of their nutritional profile. Furthermore, the capacity to modulate the structure of cocoa spreads by varying the bioaerogel content, would allow the formulation of spreads tailored for specific uses.

Noteworthily, the proposed formulation approach revealed high efficiency since an incredibly low amount of bioaerogel particles was required for spread formulation, possibly offering a competitive advantage over other ingredients exerting an oil structuring effect at higher concentrations. Additionally, the preliminary technical and economic feasibility assessment indicated a strong potential for industrial scale production of bioaerogels from plant tissues.

These outcomes pave the way to the development of feasible new functional food ingredients that align with both consumer health and environmental goals.

Fundings

This work was financed by the EU- NextGenerationEU Project "UNITED - SUstainable recycliNg of fruIT pomace and substandard pulsEs towards fooD and non-food solution"; PRIN Bando 2022; Prot. 2022P8ZAHW.

This work was supported by the University of Udine in the framework of the collaborative research project UNITED (DM737).

Author Contributions

Conceptualization SP LM, Data curation LDB, LG, BS, Formal analysis LDB, LG, BS, DAM Investigation LDB, LG, BS, DAM Methodology LDB SP BS, Project administration LM, Resources LM, IS Supervision LM, IS Visualization LDB SP, Writing - original draft LDB SP, LG, BS Writing - review and editing All the authors.

Acknowledgements

The authors would like to acknowledge the support for this research provided by the COST Action CA18125 "Advanced Engineering and Research of aeroGels for Environment and Life Sciences" (AERoGELS), funded by the European Commission, as well as the Accreditation as Center of Excellence Severo Ochoa CEX2021-001189-S funded by MCIU/AEI/10.13039/501100011033.

Declarations of interest: The authors declare that they have no known competing financial interests or personal relationships that could have appeared to influence the work reported in this paper.

References

Abdullah, Zou, Y. C., Farooq, S., Walayat, N., Zhang, H., Faieta, M., Pittia, P., & Huang, Q. (2023). Bio-aerogels: Fabrication, properties and food applications. *Critical Reviews in Food Science and Nutrition*, *63*, 6687–6709. https://doi.org/10.1080/10408398.2022.2037504

Agudelo-Laverde, L. M., Schebor, C., & Buera, M. del P. (2013). Water content effect on the chromatic attributes of dehydrated strawberries during storage, as evaluated by image analysis. *LWT-Food Science and Technology*, *52*, 157–162. https://doi.org/10.1016/j.lwt.2012.06.022

Alavi, F., & Ciftci, O. N. (2023). Superlight macroporous aerogels produced from cold-set egg white protein hydrogels show superior oil structuring capacity. *Food Hydrocolloids*, *136*, 108180. https://doi.org/10.1016/j.foodhyd.2022.108180

Andlinger, D. J., Bornkeßel, A. C., Jung, I., Schröter, B., Smirnova, I., & Kulozik, U. (2021). Microstructures of potato protein hydrogels and aerogels produced by thermal crosslinking and

supercritical drying. *Food Hydrocolloids*, *112*, 106305. https://doi.org/10.1016/J.FOODHYD.2020.106305

Betz, M., García-González, C. A., Subrahmanyam, R. P., Smirnova, I., & Kulozik, U. (2012). Preparation of novel whey protein-based aerogels as drug carriers for life science applications. *The Journal of Supercritical Fluids*, *72*, 111–119. https://doi.org/10.1016/j.supflu.2012.08.019

Blake, A. I., & Marangoni, A. G. (2015). Factors affecting the rheological properties of a structured cellular solid used as a fat mimetic. *Food Research International*, *74*, 284–293. https://doi.org/10.1016/j.foodres.2015.04.045

Braybrook, S. A. (2015). Measuring the elasticity of plant cells with atomic force microscopy. *Methods in Cell Biology*, *125*, 237–254. https://doi.org/10.1016/bs.mcb.2014.10.006

Brummell, D. A. (2006). Cell wall disassembly in ripening fruit. *Functional Plant Biology*, *33*, 103–119. https://doi.org/10.1071/fp05234

Castro, R. I., Muñoz-Vera, M., & Morales-Quintana, L. (2021). Evaluation of cell wall modification in two strawberry cultivars with contrasted softness. *Agronomy*, *11*, 1100. https://doi.org/10.3390/agronomy11061100/S1

Chaka, K. T. (2022). Extraction of cellulose nanocrystals from agricultural by-products: a review. *Green Chemistry Letters and Reviews*, *15*, 582–597. https://doi.org/10.1080/17518253.2022.2121183

Ciuffarin, F., Négrier, M., Plazzotta, S., Libralato, M., Calligaris, S., Budtova, T., & Manzocco, L. (2023). Interactions of cellulose cryogels and aerogels with water and oil: Structure-function relationships. *Food Hydrocolloids*, *140*, 108631. https://doi.org/10.1016/j.foodhyd.2023.108631

Ciuffarin, F., Plazzotta, S., Gelas, L., Calligaris, S., Budtova, T., & Manzocco, L. (2024). Cellulose cryogel particles for oil structuring: Mixture properties and digestibility. *Food Hydrocolloids*, *157*, 110470. https://doi.org/10.1016/J.FOODHYD.2024.110470

De Graef, V., Depypere, F., Minnaert, M., & Dewettinck, K. (2011). Chocolate yield stress as measured by oscillatory rheology. *Food Research International*, *44*, 2660–2665. https://doi.org/10.1016/j.foodres.2011.05.009

De Vries, A., Gomez, Y. L., Van der Linden, E., & Scholten, E. (2017). The effect of oil type on network formation by protein aggregates into oleogels. *RSC Advances*, *7*, 11803–11812. https://doi.org/10.1039/c7ra00396j

Fricke, J., & Tillotson, T. (1997). Aerogels: Production, characterization, and applications. *Thin Solid Films*, *297*, 212–223. https://doi.org/10.1016/s0040-6090

Gaggero, G., Subrahmanyam, R. P., Schroeter, B., Gurikov, P., & Delucchi, M. (2022). Organic bio-based aerogel from food waste: preparation and hydrophobization. *Gels*, *8*, 691. https://doi.org/10.3390/gels8110691

García-González, C. A., Budtova, T., Durães, L., Gaudio, P. Del, Gurikov, P., Koebel, M., Liebner, F., Neagu, M., & Smirnova, I. (2019). An opinion paper on aerogels for biomedical and environmental applications. *Molecules*, *24*, 1815. https://doi.org/10.3390/molecules24091815

Gibowsky, L., De Berardinis, L., Plazzotta, S., Manke, E., Jung, I., Méndez, D. A., ... & Schroeter, B. (2025). Conversion of natural tissues and food waste into aerogels and their application in oleogelation. *Green Chemistry*, *27*, 4713 - 4731. https://doi.org/10.1039/D4GC05703A

Guichard, E., Galindo-Cuspinera, V., & Feron, G. (2018). Physiological mechanisms explaining human differences in fat perception and liking in food spreads-a review. *Trends in Food Science & Technology*, *74*, 46–55. https://doi.org/10.1016/J.TIFS.2018.01.010

Horvat, G., Pantić, M., Knez, Ž., & Novak, Z. (2022). A brief evaluation of pore structure determination for bioaerogels. *Gels*, *8*, 438. https://doi.org/10.3390/gels8070438

Jung, I., Schroeter, B., Plazzotta, S., De Berardinis, L., Smirnova, I., Gurikov, P., & Manzocco, L. (2023). Oleogels from mesoporous whey and potato protein based aerogel microparticles: Influence of microstructural properties on oleogelation ability. *Food Hydrocolloids*, *142*, 108758. https://doi.org/10.1016/j.foodhyd.2023.108758

Kikini, J. L., & Dickie, A. (1982). A model of food spreadability from fluid mechanics. *Journal of Texture Studies, 13*, 211–227. https://doi.org/10.1111/j.1745-4603.1982.tb01396.x

Kleemann, C., Schuster, R., Rosenecker, E., Selmer, I., Smirnova, I., & Kulozik, U. (2020). In-vitro-digestion and swelling kinetics of whey protein, egg white protein and sodium caseinate aerogels. *Food Hydrocolloids, 101*, 105534. https://doi.org/10.1016/j.foodhyd.2019.105534

Kurd, F., Fathi, M., Shahedi, M., & Soltanizadeh, N. (2025). Fabrication and characterization of multifunctional bioactive aerogel pads as superabsorbent-case study: Meat preservation. *Food Research International, 209*, 116268. https://doi.org/10.1016/j.foodres.2025.116268

Laxar, T. (2003). Plant physiology. 3rd edn. In *Annals of Botany* (Vol. 91, Issue 6). Oxford Academic. https://doi.org/10.1093/aob/mcg079

Manzocco, L., Barozzi, L., Plazzotta, S., Sun, Y., Miao, S., & Calligaris, S. (2024). Feasibility of water-to-ethanol solvent exchange combined with supercritical CO_2 drying to turn pea waste into food powders with target technological and sensory properties. *LWT-Food Science and Technology, 194*, 115778. https://doi.org/10.1016/j.lwt.2024.115778

Manzocco, L., Calligaris, S., Camerin, M., Pizzale, L., & Nicoli, M. C. (2014). Prediction of firmness and physical stability of low-fat chocolate spreads. *Journal of Food Engineering, 126*, 120-125. https://doi.org/10.1016/j.jfoodeng.2013.10.042

Manzocco, L., Mikkonen, K. S., & García-González, C. A. (2021). Aerogels as porous structures for food applications: smart ingredients and novel packaging materials. *Food Structure, 28*, 100188. https://doi.org/10.1016/j.foostr.2021.100188

Manzocco, L., Plazzotta, S., Powell, J., de Vries, A., Rousseau, D., & Calligaris, S. (2022). Structural characterisation and sorption capability of whey protein aerogels obtained by freeze-drying or supercritical drying. *Food Hydrocolloids, 122*, 107117. https://doi.org/10.1016/j.foodhyd.2021.107117

Mendez, D. A., Fabra, M. J., Martínez-Abad, A., Martínez-Sanz, Gorria, M., & López-Rubio, A. (2021). Understanding the different emulsification mechanisms of pectin: Comparison between

watermelon rind and two commercial pectin sources. *Food Hydrocolloids*, *120*, 106957. https://doi.org/10.1016/J.FOODHYD.2021.106957

Méndez, D. A., Schroeter, B., Martínez-Abad, A., Fabra, M. J., Gurikov, P., & López-Rubio, A. (2023). Pectin-based aerogel particles for drug delivery: Effect of pectin composition on aerogel structure and release properties. *Carbohydrate Polymers*, *306*, 120604. https://doi.org/10.1016/j.carbpol.2023.120604

Plazzotta, S., Alongi, M., De Berardinis, L., Melchior, S., Calligaris, S., & Manzocco, L. (2022). Steering protein and lipid digestibility by oleogelation with protein aerogels. *Food & Function*, *13*, 10601–10609. https://doi.org/10.1039/d2fo01257j

Plazzotta, S., Calligaris, S., & Manzocco, L. (2018). Innovative bioaerogel-like materials from fresh-cut salad waste via supercritical-CO_2-drying. *Innovative Food Science & Emerging Technologies*, *47*, 485–492. https://doi.org/10.1016/j.ifset.2018.04.022

Plazzotta, S., Calligaris, S., & Manzocco, L. (2020). Structural characterization of oleogels from whey protein aerogel particles. *Food Research International*, *132*, 109099. https://doi.org/10.1016/j.foodres.2020.109099

Plazzotta, S., Calligaris, S., & Manzocco, L. (2023). Feasibility of protein aerogel particles as food ingredient: The case of cocoa spreads. *Journal of Food Engineering*, *351*, 111522. https://doi.org/10.1016/j.jfoodeng.2023.111522

Plazzotta, S., De Berardinis, L., Schroeter, B., & Manzocco, L. (2025). Development of novel microaerogel particles from pea protein and their application as ingredient for low-saturated fat cocoa spreads. *Journal of Food Engineering*, *391*, 112413. https://doi.org/10.1016/j.jfoodeng.2024.112413

Plazzotta, S., Jung, I., Schroeter, B., Subrahmanyam, R. P., Smirnova, I., Calligaris, S., Gurikov, P., & Manzocco, L. (2021). Conversion of whey protein aerogel particles into oleogels: Effect of oil type on structural features. *Polymers*, *13*, 4063. https://doi.org/10.3390/polym13234063/S1

Rincon Cardona, J. A., Huck, C., & Lidia, M. (2013). Applications of confocal laser scanning microscopy (CLSM) in foods. In: Lagali, N. (ed) Confocal Laser Microscopy - Principles and Applications in Medicine, Biology, and the Food Sciences. https://doi.org/10.5772/55653

Rousseau, D., Coutouly, A., Hendricks, P., Hodge, S., & Green, N. L. (2015). Development of an extraction protocol for the removal of the fat phase within chocolate. *LWT-Food Science and Technology*, *64*, 61–66. https://doi.org/10.1016/j.lwt.2015.05.019

Saeman, J. F. (1945). Kinetics of wood saccharification - hydrolysis of cellulose and decomposition of sugars in dilute acid at high temperature. *Industrial & Engineering Chemistry*, *37*, 43–52. https://doi.org/10.1021/IE50421A009

Schroeter, B., Jeansathawong, P., Hajnal, A., & Gurikov, P. (2023). Wet milling of alginate alco- and hydrogel composites: A Facile top-down approach for continuous production of aerogel microparticles. *Macromolecular Materials and Engineering*, *308*, 2200674. https://doi.org/10.1002/mame.202200674

Selmer, I., Karnetzke, J., Kleemann, C., Lehtonen, M., Mikkonen, K. S., Kulozik, U., & Smirnova, I. (2019). Encapsulation of fish oil in protein aerogel micro-particles. *Journal of Food Engineering*, *260*, 1–11. https://doi.org/10.1016/j.jfoodeng.2019.04.016

Sharma, P., Venugopal, A.P. (2023). Bruise damage susceptibility of blueberry and strawberry. In: Pathare, P.B., Opara, U.L. (eds) Mechanical Damage in Fresh Horticultural Produce. Springer, Singapore. https://doi.org/10.1007/978-981-99-7096-4_12

Suutarinen, J., Änäkäinen, L., & Autio, K. (1998). Comparison of light microscopy and spatially resolved fourier transform infrared (FT-IR) microscopy in the examination of cell wall components of strawberries. *LWT-Food Science and Technology*, *31*, 595–601. https://doi.org/10.1006/fstl.1997.0331

Suutarinen, J., Honkapää, K., Heiniö, R. L., Autio, K., & Mokkila, M. (2000). The effect of different prefreezing treatments on the structure of strawberries before and after jam making. *LWT-Food Science and Technology*, *33*, 188–201. https://doi.org/10.1006/fstl.2000.0638

Taghavi, T., Patel, H., & Rafie, R. (2023). Extraction solvents affect anthocyanin yield, color, and profile of strawberries. *Plants*, *12*, 1833. https://doi.org/10.3390/plants12091833/S1

Thommes, M., Kaneko, K., Neimark, A. V., Olivier, J. P., Rodriguez-Reinoso, F., Rouquerol, J., & Sing, K. S. W. (2015). Physisorption of gases, with special reference to the evaluation of surface area and pore size distribution (IUPAC Technical Report). *Pure and Applied Chemistry*, *87*, 1051–1069. https://doi.org/10.1515/pac-2014-1117

Wu, D. T., Li, W. X., Wan, J. J., Hu, Y. C., Gan, R. Y., Zou, L. A., Wu, D. T., Li, W. X., Wan, J. J., Hu, Y. C., Gan, R. Y., & Zou, L. (2023). A comprehensive review of pea (Pisum sativum L.): Chemical composition, processing, health benefits, and food applications. *Foods*, *12*, 2527. https://doi.org/10.3390/foods12132527

Wu, Y., Li, B. H., Chen, M. M., & Bing, L. (2024). An aerogel-based intelligent active packaging with the dual functions of spoilage detection and freshness preservation. *Food Hydrocolloids*, *156*, 110160. https://doi.org/10.1016/j.foodhyd.2024.110160

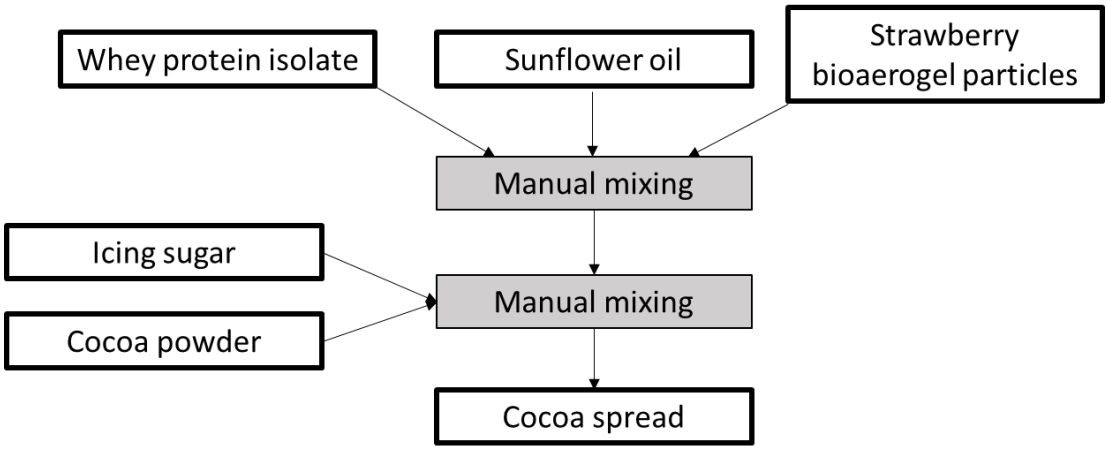

Figure 1. Flowchart for the preparation of cocoa spreads.

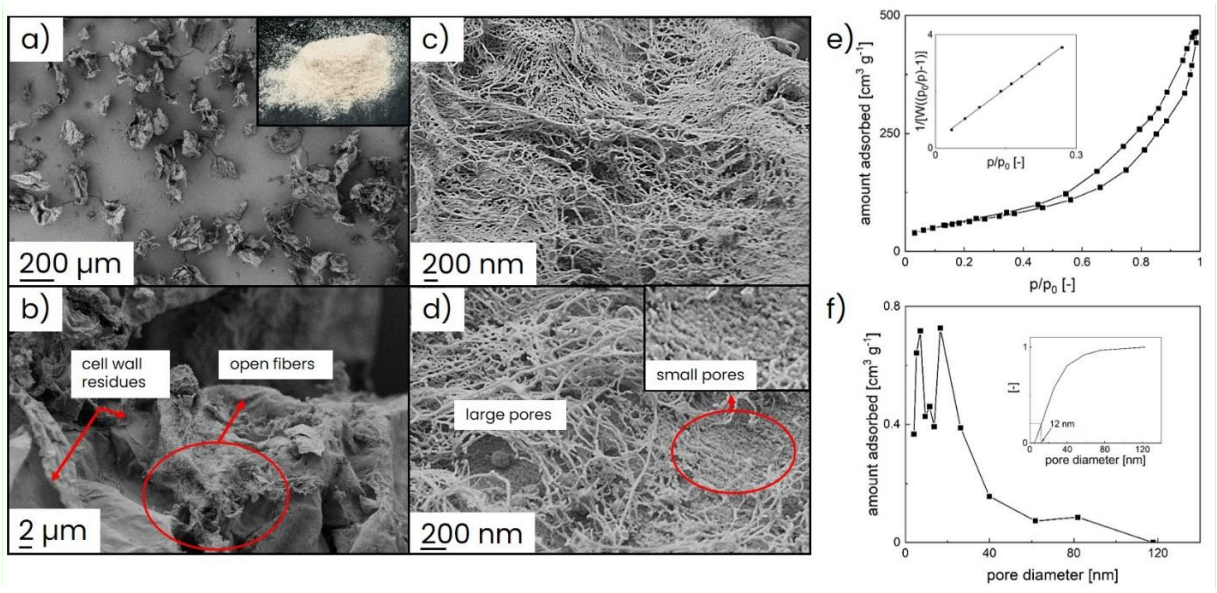

Figure 2 a) – d) SEM images of aerogel particles produced by water-to-ethanol solvent exchange, colloidal milling and supercritical-CO_2-drying of strawberry pulp, taken at different magnifications, a) 500x, inset: photographic image of the powder; b) 5000x; c) 50000x; d) 100000x. e) N_2-isotherm, the inset depicts the BET-plot used for estimation of the specific surface area (R^2=0.9999). f) Mesopore size distribution, estimated via BJH method. The inset represents the normalized cumulative mesopore volume.

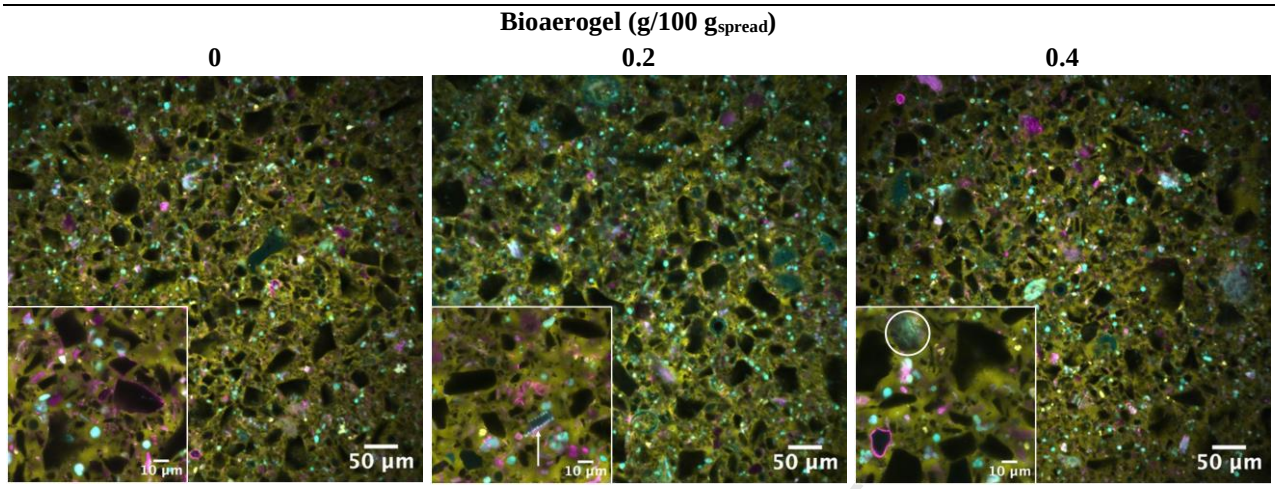

Figure 3. Confocal micrographs of cocoa spreads obtained by partially substituting whey protein isolate with increasing amounts of strawberry bioaerogel particles (0, 0.2 and 0.4 g/100 g$_{spread}$). Black: sugar; magenta: whey protein isolates; fluorescence: cocoa powder or strawberry bioaerogel particles. White arrow: bioaerogel particle with tracheids structure; white circle: bioaerogel particle with irregular shape.

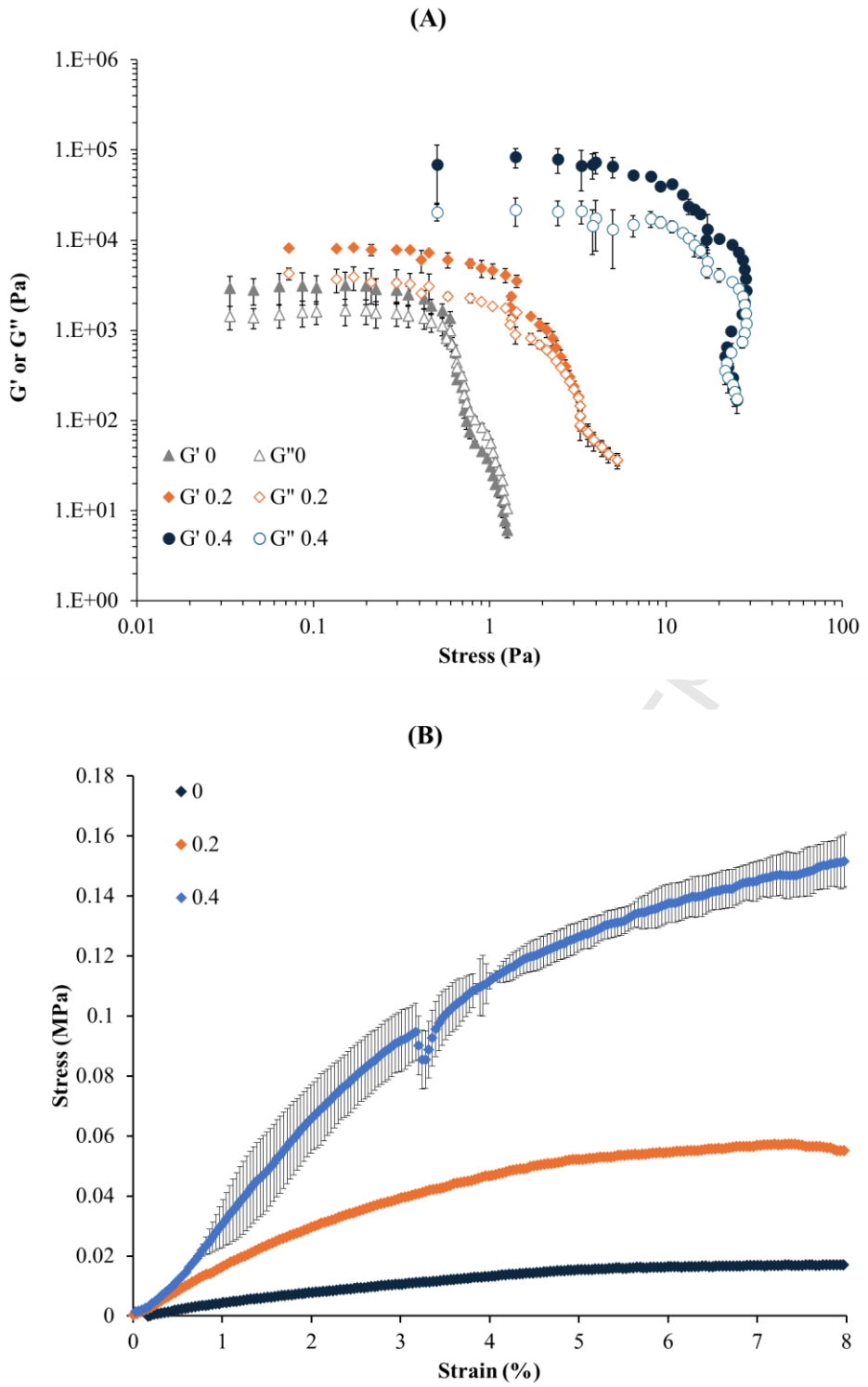

Figure 4. Amplitude sweep (A) and spreadability (B) test of cocoa spreads obtained by partially substituting whey protein isolate with increasing amounts of strawberry bioaerogel particles (0, 0.2 and 0.4 g/100 g_{spread}).

Declaration of interests

☒ The authors declare that they have no known competing financial interests or personal relationships that could have appeared to influence the work reported in this paper.

☐ The authors declare the following financial interests/personal relationships which may be considered as potential competing interests:

Graphical abstract

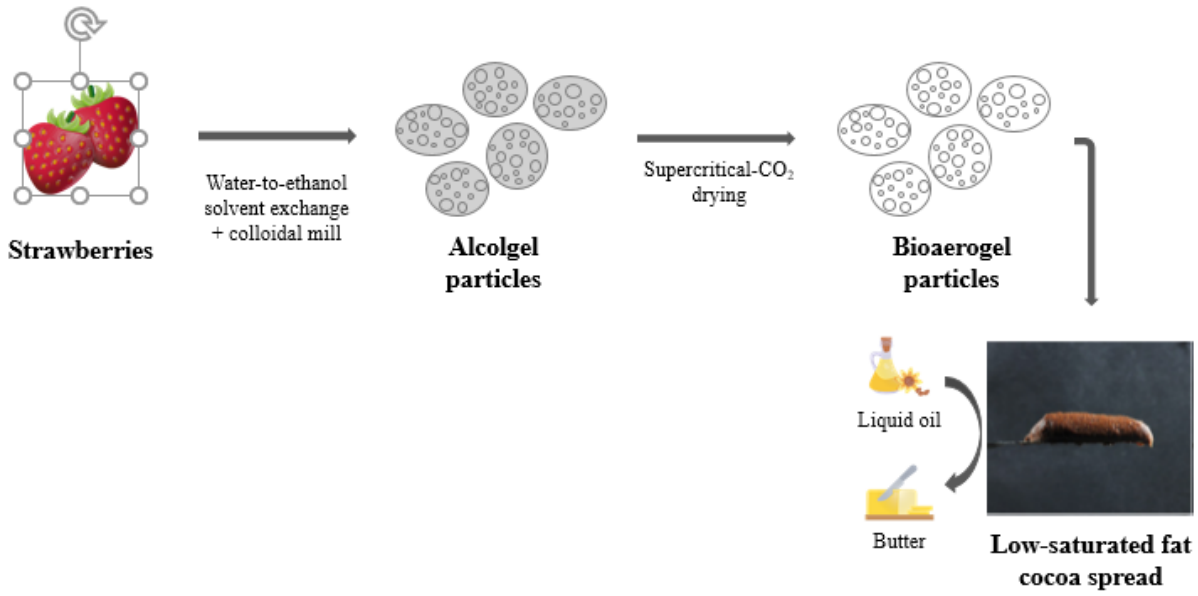

Highlights

- Bioaerogel particles were efficaciously produced directly from strawberries (SB)
- Mesoporous particles (0.69 cm^3 g^{-1}) with high surface area (233 m^2 g^{-1}) were obtained
- The SB-derived bioaerogel particles revealed high oil absorption exceeding 90% w/w
- Low-saturated-fat spreads were obtained using SB particles as structuring ingredients
- The spread physical properties could be adjusted by varying the SB bioaerogel content